STRUCTURAL AND MICROSTRUCTURAL STUDY OF GAMMA RAY-IRRADIATED CO-DOPED BARIUM TITANATE ($Ba_{0.88}Ca_{0.12}Ti_{0.975}Sn_{0.025}O_3$)

Umaru Ahmadu[1], Ahmad Abubakar Soje[2], Abdulwaliyu Bidemi Usman[1],
Auwal Muhammad Musa[3], Kasim Uthman Isah[1]
[1]Department of Physics, Federal University of Technology, P.M.B., 65, Minna, Nigeria
[2]College of Agriculture P.M.B.109, Mokwa, Niger State, Nigeria
[3]Centre for Energy Research and Training (CERT), Zaria, Nigeria

[1]u.ahmadu@ yahoo.com
[2]ahmadsoje@ gmail.com

Abstract
Barium calcium stannate titanate ($Ba_{0.88}Ca_{0.12}Ti_{0.975}Sn_{0.025}O_3$) ceramics, synthesized by solid state reaction method and sintered at 1100 °C/3 h, were exposed to gamma radiation dose of up to 1 kGy using a Cs-137 irradiation source at a dose rate of 100.46Gy/h. Structural analysis of the ceramics indicated a tetragonal perovskite crystalline structure for both pristine and irradiated ceramics with a minor secondary phase. However, slight changes of the lattice parameters and average crystallite size were observed for the irradiated samples. The lattice aspect ratio of the tetragonal phase (c/a) for the pristine ceramics was 1.0022 which decreased by 0.22% at maximum irradiation dose. Irradiation also causes some microstructural changes and slight decrease in grain size. Energy dispersive spectroscopic investigation of the $Ba_{0.88}Ca_{0.12}Ti_{0.975}Sn_{0.025}O_3$ showed small variation in its chemical composition as gamma radiation dose is increased.

Keywords: ceramics, gamma radiation, grain size, lattice parameters, surface morphology

1. Introduction
Barium titanate ($BaTiO_3$ or BT) has been used in capacitors, ultrasonic transducers, pyroelectric infrared sensors, and positive temperature coefficient (PTC) resistors (Fisher *et al.*, 2013; Sheela *et al*, 2010). BT is in ferroelectric perovskite (ABO_3) tetragonal phase from room temperature up to the Curie temperature (Tc,120 °C) (Fratini *et al.*, 2012) above which it transforms to paraelectric-cubic phase (Sheela *et al*, 2010). However, there are few drawbacks, such as low piezoelectric constants and structural phase transformations at low temperatures which limit the extensive application of the pure BT in piezoelectric devices (Aksel *et al.*, 2010).

2. Literature Review
In recent years, there have been several attempts at improving its structural stability alongside other properties, such as ferroelectric and dielectric constants (Cai *et al.*, 2011, Chen *et al.*, 2012, Lijuan *et al.*, 2013, Choudhury *et al.*, 2008, Dash *et al.*, 2014 Rao *et al.*, 2013, Kim *et al.*, 2009, Saikat *et al.*, 2013, Kumar *et al.*, 2009 and Dughaish *et al.*, 2013).
Such attempts include the substitution of Ba^{2+} or Ti^{4+} by atoms of different sizes and oxidation states resulting in compounds of different physical and chemical properties, while still retaining the same structural phase (Chen *et al.*, 2012, Lijuan *et al.*, 2013, Choudhury *et al.*, 2008, Dash *et al.*, 2014, Rao *et al.*, 2013, Kim *et al.*, 2009, Saikat *et al.*, 2013, Kumar *et al.*, 2009, Dughaish *et al.*, 2013, and Vitayakorn *et al.*, 2016). The substitution on the A-site of BT (Ba^{2+}) by Ca^{2+} by up to 0.12mol prevents grain growth, improves electromechanical properties, structural stability (Choi *et al.*, 2010, Paunovic *et al.*, 2004, and Matsuura *et al.*, 2014) and decreases dielectric constant (Vitayakorn *et al.*, 2016, Choi *et al.*, 2010., and Paunovic *et al.,* 2004). On the other hand, substitution of the B-site (Ti^{4+}) by Sn^{4+} (0.025mol) increases permittivity and piezoelectric properties, but decreases the Tc (Nath and Medhi, 2012). Therefore, it is expected that simultaneous substitutions of Ba^{2+} by Ca^{2+} and Ti^{4+} by Sn^{4+} could lead to a piezoelectric ceramics having high permittivity, improved piezoelectric properties and structural stability.
Barium titanate-based materials have potential applications in nuclear radiation environments such as sensors in nuclear reactors, particle accelerators, detectors, space ship and satellites, among others (Medhi and Nath, 2013). The properties of such materials used in the fabrication of devices deployed in these environments should not be affected by nuclear radiation. Nuclear radiations, particularly gamma rays are of significant concern because they readily penetrate through protective shielding. The ionizing effect of gamma radiation may alter the structurally dependent properties of materials and hence their performance. The magnitude of such changes is largely dependent on radiation parameters such as linear energy transfer, dose and energy, nature of the material and its structural phase (Ogundare *et al.*, 2016). However, the semiconducting and dielectric properties of BT ceramics have been found to depend on grain size and phase content (Hsiang *et al.*, 1996).
Recently, it was reported that structural properties of BT-based ceramics were altered on exposure to gamma radiation dose of up to 200Gy (Medhi and Nath, 2013, Nath and Medhi 2015) with subsequent decrease in grain size. Moreover, works on higher gamma ray exposure (dose) of BT-based ceramics is sparse in literature and extensive literature survey has revealed that so far, no work has been reported on gamma ray irradiated $Ba_{0.88}Ca_{0.12}Ti_{0.975}Sn_{0.025}O_3$ ceramics to the best of our knowledge. This work therefore aims to study the effect of gamma radiation on the microstructure of $Ba_{0.88}Ca_{0.12}Ti_{0.975}Sn_{0.025}O_3$ ceramics which might provide information on the stability of BT based devices for applications in space and radiation environments.

3. Methodology

$Ba_{0.88}Ca_{0.12}Ti_{0.975}Sn_{0.025}O_3$ (BCST) ceramics has been synthesized by solid state reaction method. Appropriate proportion of analytical grade $BaCO_3$ (≥99%, Kermel, China), TiO_2 and $CaCO_3$ (99.9%, Qualikems, India) and SnO_2 (99.99%, BDH, UK) were manually mixed thoroughly in an agate mortar and distilled water was added to the mixture to form a slurry in order to prevent selective sedimentation of the reagents. The slurry was dried in an oven at 150 °C for 1 hour and hand-ground using an agate mortar and pestle for about 4 hours to achieve homogeneity of the mixture. The homogenous mixture was placed in an alumina crucible and calcined at 1050 °C for 4 hours in a furnace to allow volatilization of bye-product, CO_2. The powder was further crushed for 1 hour and ground by adding 4wt% polyvinyl alcohol (PVA) as a binder before forming pellets. The pellets with diameter and thickness of 26mm and 1mm, respectively, were obtained at a pressure of 10 tons using a MiniPal4 Pw 4025/47B palletizing machine. The pellets were sintered at 1100 °C for 3 hours, and furnace-cooled for crystal phase formation. The sintered pellets were irradiated with gamma ray doses of 0.1, 0.3, 0.5, 0.7 and 1 kGy (the samples were labelled as BCST-0.1, BCST-0.3, BCST-0.5, BCST-0.7 and BCST- 1, respectively) using a Cesium-137 (Cs-137) irradiation source at a dose rate of 100.46Gy/h.
X-ray diffractometer (D8 Advance, Bruker AXS,40 kV,40mA) with monochromatic Cu-K_α (λ=1.54060Å) was used to characterize the structural phase composition of the pristine and irradiated ceramics. The instrument was operated in a step scan mode of size 0.034° and counts were accumulated for 88 s at each step for 2θ angles ranging from 20° to 90°. The ceramics were positioned on an aluminium stage with the aid of carbon adhesive tape and coated with AuPd (goldpalladium) using a sputter coater. Their surface morphology and elemental compositions were investigated using a high resolution scanning electron microscope (HRSEM, Zeiss) coupled with an EDS spectrometer. The HRSEM was operated at a voltage of 20 kV and images captured at 5 kV.

4. Results and Discussion

4.1. *Crystal Structure and Parameters*

Typical X-ray diffraction (XRD) patterns of the synthesized $Ba_{0.88}Ca_{0.12}Ti_{0.975}Sn_{0.025}O_3$ (BCST) ceramics at room temperature and irradiated with varying gamma ray doses are shown in Fig. 1. The prominent peaks in the XRD spectra correspond to the tetragonal phase of $BaTiO_3$ and matches well with JCPDS No. 00-005-0626 data. The XRD patterns are in agreement with reports of other groups who prepared BT-based ceramics using similar method (Rao *etal.*, 2013 and Fasasi *etal.*, 2006).

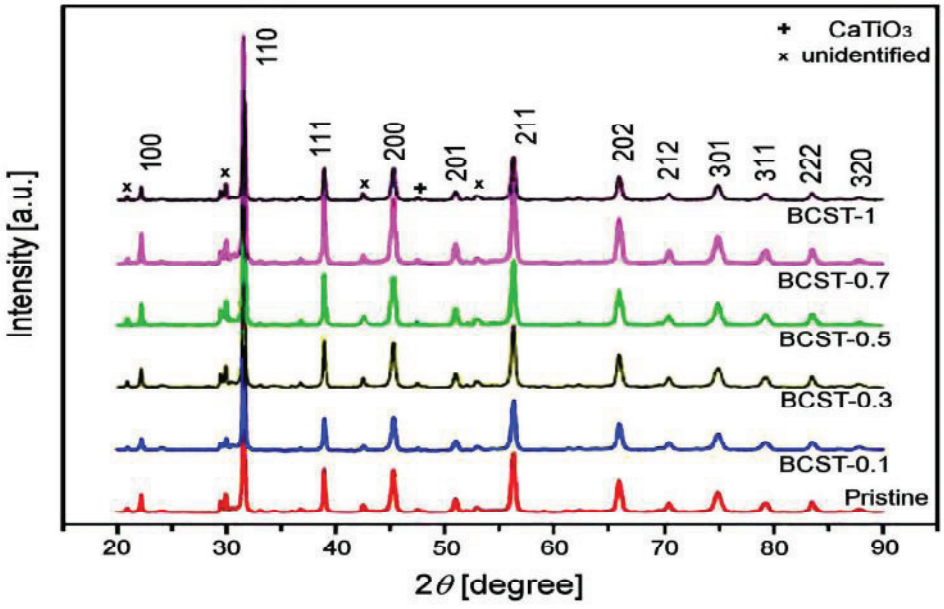

Figure 1. X-ray Diffraction Patterns of Pristine and Irradiated BCST Ceramic

Table 1. XRD Data (2θ Position (200), *d*-Spacing and FWHM) for the Peak 200 of Pristine and Irradiated BCST Ceramic

Sample	2θ	d-Spacing	FWHM
BCST	45.261	2.0019	0.410
BCST-A	45.285	1.9884	0.407

BCST-B	45.266	2.0017	0.418
BCST-C	45.278	2.0012	0.405
BCST-D	45.276	2.0013	0.397
BCST-E	45.270	2.0029	0.391

However, a minor peak around 47.5° 2θ can be observed and identified as orthorhombic $CaTiO_3$ phase (JCPDS file No. 00-022-0153). There were other diffraction peaks though with very low intensities whose match could not be found as indicated in the XRD spectra. The XRD pattern of the irradiated ceramics suggests a consistent phase and composition with the pristine sample. This corroborates the fact that gamma radiation does not change the perovskite structure of barium titanate based ceramics. Similar observations have been reported previously (Medhi and Nath, 2013, Nath and Medhi 2015).

Table 1 gives a quantitative analysis of the peak positions and parameters of the XRD patterns where the d values were obtained experimentally. It is observed that as the irradiation dose increases the structure sensitive XRD peak 200 slightly shifts towards higher 2θ angles. This can be discerned from the raw XRD data (not shown). Similar pattern has been observed when the A site of a typical ABO_3 structure is partially replaced by ions of smaller size (Chen *etal.*, 2012, and Yun *etal.*, 2007) and leads to distortion of the ABO_3 unit cell lattice (Chen *etal.*, 2012) together with changes in the lattice parameters. Therefore, the slight shift of peaks to higher angles may be attributed to A-site defects due to the energetic gamma ray.

The average crystallite sizes (D) of the pristine and irradiated ceramics were calculated using the full width at half maximum (FWHM) of the most intense peak by the Scherrer formula (Dash *etal.*, 2014):

$$D = 0.9\lambda/\beta cos\theta \qquad (1)$$

where β is the FWHM of the diffraction peak in radians, θ the Bragg diffraction angle, λ the wavelength of the X-ray used and D the average crystallite size.

The calculated average crystallite size of the pristine ceramic is found to be approximately 38 nm. It can be seen from the plot of β and D versus irradiation dose (Fig. 2) that β values of the pristine increased while D values decreased on exposure to lower dose (up to 0.5 kGy). However, on further increasing the dose up to 1 kGy, β and D appear to be almost the same with the corresponding values for the pristine sample.

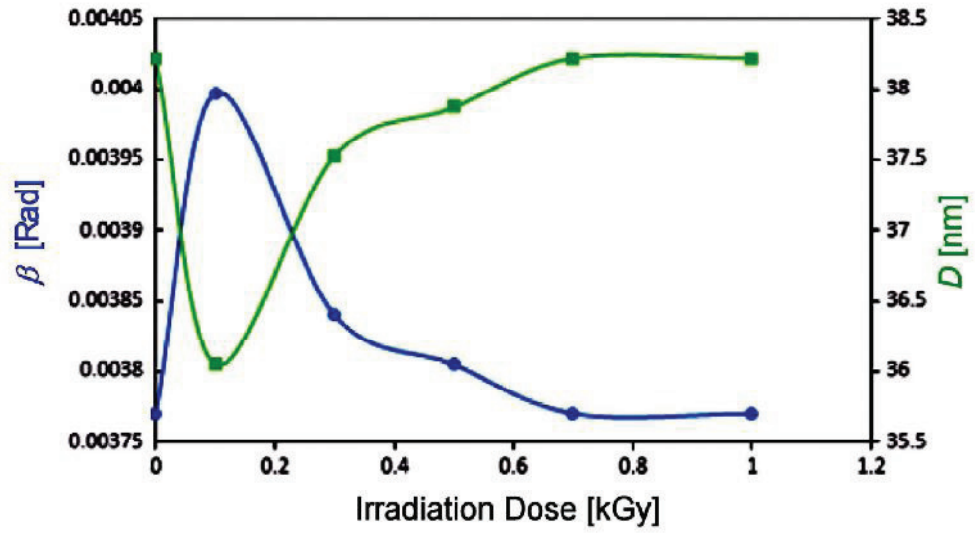

Figure 2. Variation of β and D against Irradiation Dose

Lattice parameters a and c of the pristine and irradiated ceramics were calculated from the XRD spectra using 100, 200 and 201 diffraction peaks. The calculated lattice aspect ratio of tetragonal phase (c/a = 1.0022) indicates a weak tetragonality of the pristine BCST ceramics in comparison with the referenced JCPDS data of BaTiO3 (c/a = 1.0110) prepared at higher temperature. Plot of lattice parameters (a and c) and c/a against irradiation dose is shown in Fig. 3. As can be seen, both a and c parameters are slightly changed, resulting in an increase of c/a ratio on exposure to lower irradiation dose (0.1 kGy). However, a value remained almost unchanged while the c values slightly decreased and consequently c/a ratio decreased with further increase in the irradiation dose. These results indicate a decrease in tetragonality of the perovskite structure of BCST ceramics upon gamma exposure. The variations in the lattice parameters can be understood in terms of the energy exchange between the gamma ray and

the lattice sites of some host atoms thereby leading to lattice distortion. This is consistent with the slight shift in peak positions to higher 2θ values. The increase in tetragonality is desirable in perovskite titanates because it increases polarizability and consequently leads to improved ferroelectric properties (Mady *etal.*, 2011). However, the observed changes indicate on higher tendency towards phase transformation in the BCST ceramics on exposure to higher gamma irradiation dose (up to 1 kGy). Thus, it is expected that irradiation would ensue deterioration in ferroelectric properties of the BCST ceramics.

The unit cell volume is another structural parameter that can be used to indicate change in the structure of a crystal (Hsiang *etal.*, 1996).The cell volume of the pristine ceramics was found to be 64.20Å^3. After gamma ray exposure, there were slight decreases of the cell volume. This is also consistent with the fact that energetic gamma rays possess the ability of ionizing the atoms of a material thereby resulting in electron-hole pairs. The observed decrease of the cell volume is corroborated by the slight shift of the XRD peak 200 toward higher angles with increasing gamma irradiation.

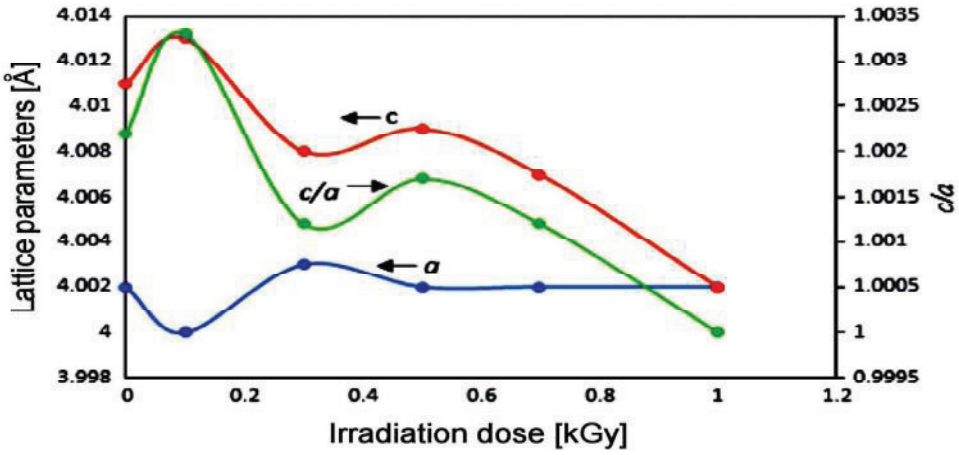

Figure 3. Variation of Lattice Parameters (a and c) and c/a Versus Irradiation Dose

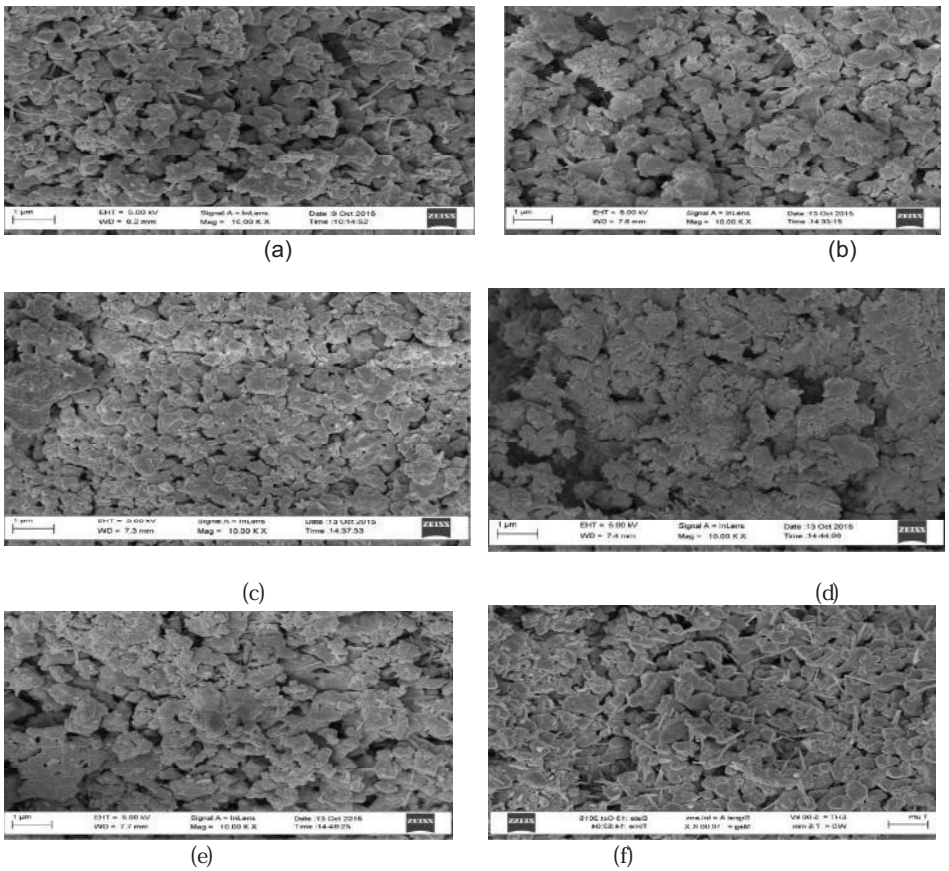

Figure 4. SEM Micrograph of: (a) BCST, (b) BCST-0.1, (c) BCST-0.3, (d) BCST-0.5, (e) BCST-0.7 and (f) BCST-1

Figure 5. Variation of Average Grain Size with Irradiation Dose

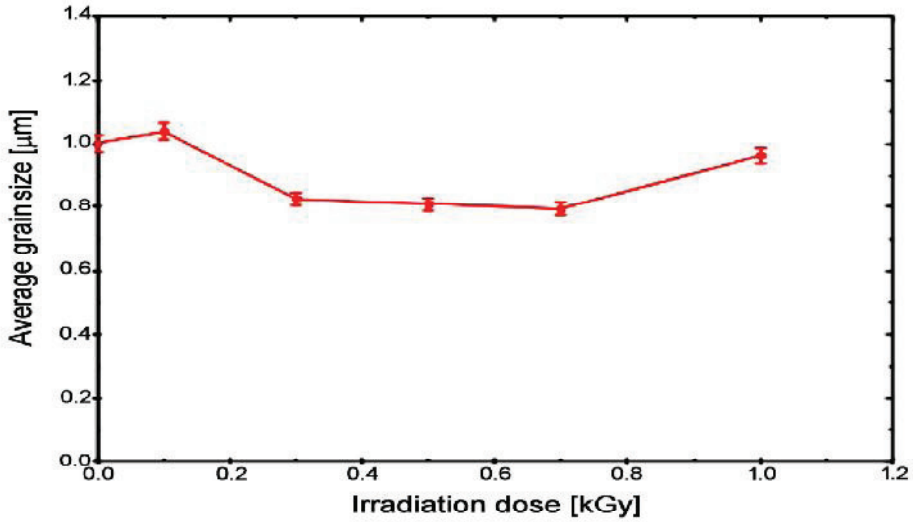

4.2.

Microstructural Analysis

Microstructural characterization of the pristine and irradiated BCST ceramics is depicted in Fig. 4. As can be seen from SEM micrograph of the pristine ceramics (Fig. 4a), there is non uniform distribution of grains. The pristine BCST ceramics contains two distinguishable microstructural features: i) a portion of agglomerates and some fairly fine grained microstructure and ii) a small portion of rod-like grains which could be attributed to rich Ca^{2+} regions necessitated by insufficient homogenization of the starting precursors (Paunovic *etal.*, 2004). Further, the presence of some residual porosity is also evident. The average grain size as determined using ImageJ software is approximately 1.0 μm based on 100 grains. It is known that the initial powder preparation process and sintering temperature could result in inhomogeneous microstructure.

SEM micrographs reveal that gamma ray affects microstructure of the BCST ceramics, especially in the aspect of distribution of grain and average grain size (Fig.4). Thus, in the samples irradiated with lower gamma ray doses (0.1 to 0.7 kGy) rod-like grains are less visible and harder agglomeration of grains become more evident (Fig. 4). However, further increase in the irradiation dose (1 kGy) results in formation of BCST structure with higher portion of rod-like grains and fairly fined-grained microstructure (Fig. 4f). This result suggests that irradiation dose at this level affects the uniformity of the composition thereby leading to segregation in local part of the ceramic.

The determined average grain sizes of the irradiated samples are depicted in Fig. 5. As can be seen there is a small variation in the average grain. These variation in the average grain size could be due to fractured grains as a result of irradiation effect. The average grain size slightly increased after exposure to lower dose (0.1 kGy), but with further increase of irradiation dose thegrainsizedecreases.

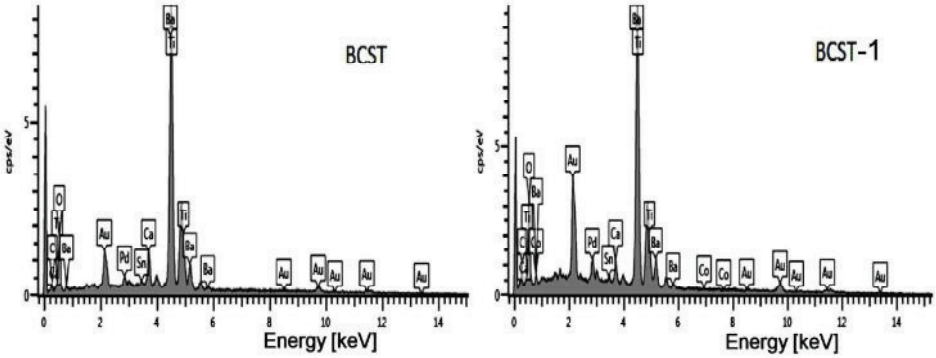

Figure 6. EDS Spectra of (a) Pristine BCST and (b) BCST-1 Ceramics

This result indicates that the average grain size of the BCST ceramics does not change considerably upon gamma ray exposure of up to 1 kGy and is contrary to some literature data (Medhi and Nath, 2013 and Nath and Medhi, 2014). However, grain size is closely connected with ferroelectric and piezoelectric properties of BT-based ceramics (Nath and Medhi, 2014). Ferroelectric and piezoelectric properties decrease when grain size decreases.

Thus, slight degradation of ferroelectric and piezoelectric properties is expected for the prepared BCST ceramic within the range of studied doses.

Table 2 Elemental Composition, Nominal Composition, Normalised EDS Derived Composition of Pristine and Irradiated BCST Ceramics

Samples	Ba	Ca	Sn	Ti	O	Total	Ba	Ca	Ti	Sn	O	Al	Co	Total
BCST	17.60	2.4	0.5	19.50	60	100.00	22.31	4.7	0.4	26.64	45.95	0.97	-	100
BCST-0.1	17.60	2.4	0.5	19.50	60	100.00	19.03	4.7	22.83	0.39	52.89	-	-	100
BCST-0.3	17.60	2.4	0.5	19.50	60	100.00	22.54	4.13	24.25	0.57	46.71	1.82	-	100
BCST-0.5	17.60	2.4	0.5	19.50	60	100.00	18.34	6.98	21.55	0.50	52.64	-	-	100
BCST-0.7	17.60	2.4	0.5	19.50	60	100.00	24.30	2.87	27.00	0.72	45..12	-	-	100
BCST-1	17.60	2.4	0.5	19.50	60	100.00	19.3	2.19	22.29	0.51	55.52	0.18	0.24	100

4.3. *Chemical Composition*

Figure 6 depicts the EDS spectra showing the elemental composition of the pristine BCST ceramics. All of the peaks have been identified with the potential elements that match that peak. The spectra clearly indicate the presence of Ba, Ca, Ti, Sn, O, C, Au and Pd. The carbon (C) source could be traced to the carbon tape and AuPd (gold-paladium) is present in the compound in order to make it conducting.

Table 2 gives a quantitative comparison between the nominal and the normalized EDS derived composition of the pristine and irradiated BCST ceramics, where the major sources of error were removed and the remaining elements normalized to 100% to give a better relative representation of the remaining elements present in the material. However, trace amount of Al and Co were evident in the samples irradiated with 0.3 and 0.1 kGy, respectively. The presence of Al could be attributed to contamination during the processing of the material for SEM analysis and the presence of Co is not understood at present. The fluctuations in the normalized EDS derived composition in comparison with the nominal composition could be attributed to deficiency of oxygen during sintering in the ambient and difficulties in achieving macroscopic uniformity in solid state reaction method (Badapanda *et al.*, 2010). A significant overlap for Ba and Ti is obvious in the spectra and makes it difficult to differentiate between them in the quantification results and this has been already reported (Korkmaz *et al.*, 2012).

5. Conclusions

$Ba_{0.88}Ca_{0.12}Ti_{0.975}Sn_{0.025}O_3$ ceramics, prepared by solid state reaction and sintering at 1100 °C/3 h, were exposed to gamma radiation dose of up to 1 kGy. The pristine BCST ceramics has polycrystalline tetragonal structure with minor impurity $CaTiO_3$ phase. Gamma irradiation does not change the perovskite structure, but the structure sensitive 200 peak was found to shift to higher 2θ angles with increase in irradiation dose. It was also observed that the crystallite size decreases on exposure to irradiation dose up to 0.5 kGy and is almost the same with further increase of dose up to 1 kGy. XRD analysis indicates on decrease in the tetragonality of the perovskite BCST structure upon gamma irradiation, which is expected to lead to deterioration in the ferroelectric properties. The microstructure of the pristine BCST ceramics is characterized by agglomerates, rod-like grains and porosity with an average grain size of ~1.0 μm. In the samples irradiated with lower gamma dose (0.1 to 0.7 kGy) rod-like grains are less visible compared to those irradiated with higher dose (1 kGy).

It was observed that the average grain size of the BCST ceramics does not change appreciably upon gamma irradiation of up to 1 kGy. However, a slight degradation in ferroelectric and piezoelectric properties is expected.

References

Aksel, E and Jones, J. L. (2010), Advances in Lead-Free Piezoelectric Materials for Sensors and Actuators, *Journal of Sensors*, Vol. 10, 1935-1954.

Badapanda, T. (2010), Structural, Electrical and Optical Study of 'A' Site Deficient Heterovalent Ion Doped Barium Zirconium Titanate Perovskite. Doctoral Thesis *National Institute of Technology,* Rourkela-769008, Orissa India, 6-58.

Cai, W., Fu1, C. L., Gao, J. C., and Zhao, C. X. (2011), Dielectric Properties and Microstructure of Mg Doped Barium Titanate Ceramics, *Journal of Advances in Applied Ceramics,* Vol. 110 (3), 181 – 185.

Chen, Z. and Yuan-Fang, Q.U. (2012), Dielectric Properties and Phase Transitions of La2O3- and Sb2O3-Doped Barium Strontium Titanate Ceramics, *Transition of Nonferrous Meterial Society China,* Vol. 22, 2742–2748.

Choi, Y. K., Hoshina, .T., Takeda, H., and Tsurumi, T. (2010), Effects of Ca and Zr Additions and Stoichiometry on the Electrical Properties of Barium Titanate-Based Ceramics, *Journal of the Ceramic Society of Japan,* Vol. 118(10), 881-886.

Choudhury, S., Akter, S., Rahman, M.J., Bhuiyan, A.H. Rahman, S.N., Khatun, N., and Hossain, M.T. (2008), Structural, Dielectric and Electrical Properties of Zirconium Doped Barium Titanate Perovskite, *Journal of Bangladesh Academic of Sciences,* Vol. 32, 151–159.

Dash, S.K., Kant, S., Danlai, B., Swain, M.D., and Swain, B.B. (2014), Characterization and Dielectric Properties of Barium Zirconium Titanate Prepared by Solid State Reaction and High Energy Ball Milling Processes, *Indian Journal of Physics*, Vol. 88(2),129–135

Dughaish, Z. H. (2013), Dielectric Properties of $(BaTiO_3)_{(1-x)}$ $(SnO_2)_x$ Ceramics, *Journal of Natural Sciences and Mathematics Qassim University*, Vol. 6(2), 107-121.

Fasasi, A.Y., Balogun, F. A., Fasasi, M. K., Ogunyele, P. O., Mokobia, C.E., and Inyang, E.P. (2006), Thermoluminescence Properties of Barium Titanate Prepared by Solid-State Reaction, *Journal of Science Direct Sensors and Actuators* Vol. A 135, 598-604.

Fisher, J.G., Lee, D., Oh J., Kim, H., Nguyen D., Kim, J., Lee, S., and Lee, H. (2013), Low Temperature Sintering of Barium Calcium Zirconium Titanate Lead-Free Piezoelectric Ceramics, *Journal of Korean Ceramic Society*, Vol. 50(2), 157–162.

Frattini, A., Di Loreto, A., de Sanctis, O., and Benavidez, E. (2012), BCZT Ceramics Prepared from Activated Powders, *Procedia Material Sci*ence, Vol. 1, 359–365.

Hsiang, H.I., Yen, F.S., and Chang, Y.H. (1996), Effects of Doping with La and Mn on the Crystallite Growth and Phase Transition of BaTiO3 Powders, *Journal of Material Sciences*, Volume 31, 2417–2424.

Kim, Y. J., Hyun, J.W., Kim, H.S., Lee, J.H., Yun, M.Y., Noh, S.J., and Ahn, Y. H. (2009), Microstructural Cheracterization Dielectric Properties of Barium Titanate Solid Solutions with Donor Dopants, *Bull Korea Chemistry Soc*iety, Vol. 30(6), 1267-1273.

Korkmaz, E. and Kalaycioglu N.O. (2012), Synthesis and Luminescence Properties of $BaTiO_3$: RE (RE=Gd^{3+},Dy^{3+},Tb^{3+},Lu^{3+}) Phosphors. *Bull Material Sciences,* Vol. 35(6), 1011-1017.

Kumar, Y., Mohiddon, M. A., Srivastava, A., and Yadav, K. L. (2009), Effect of Doping on Structural and Dielectric Properties of $BaTiO_3$, *Indian Journal of Engineering and Materials Sciences*, Vol. 16, 390-394.

Lijuan, Z., Lihai, W., Jiandang, L., Bin, C., Minglei, Z., and Bangjiao., Y. (2013), Dielectric Properties and Structural Defects in $BaTi_{1-x}Sn_xO_3$ Ceramics, 16th International Conference on Positron Annihilation (ICPA-16), *Journal of Physics*, Conference Series 443,012014.

Mady, H.A. (2011), XRD and Electric Properties of Lead Barium Titanate Ferroelectric Ceramic, *Australian Journal of Basic Applied Sciences,* Vol. 5 (10), 1472–1477.

Matsuura, K., Hoshina, T., Takeda, H., Sakabe, Y., and Tsurumi, T. (2014), Effects of Ca Substitution on Room Temperature Resistivity of Donor-Doped Barium Titanate Based PTCR Ceramics, *Journal of the Ceramic Society of Japan*, Vol. 122(6), 402-405.

Medhi, N. and Nath, A. K. (2013), Gamma Ray Irradiation Effects on the Ferroelectric and Piezoelectric Properties of Barium Titanate Ceramics. *Journal Materials Engineering and Performance (EGJME)*, Vol. 22, 2716-2722.

[a]Nath, A. K. and Medhi, N. (2012), Density Variation and Piezoelectric Properties of $Ba(Ti_{1-x}Sn_x)O_3$ Ceramics Prepared from Nanocrystalline Powders, *Bull. Material Sciences*, Vol. 5(35), 847–852.

[b]Nath, A. K. and Medhi, N. (2015), Effect of Gamma ray Irradiation on the Piezoelectric and Ferroelectric Properties of Bismuth Doped Barium Titanate Ceramics, *Indian Journal of Physics,* Vol. 89(2), 131-136.

Ogundare, F.O. and Olarinoye, I.O. (2016), He^+ Induced Changes in the Surface Structure and Optical Properties of RF-Sputtered Amorphous Alumina Thin films, Journal of Non-Crystal Solids, Vol. 432, 292–299.

Paunovic, V., Zivkovic, L., Vracar, L., Mitic, V., and Milijkovic, M. (2004), Effects of Additive on Microstructure and Electrical Properties of $BaTiO_3$ Ceramics, *Serbian Journal of Electrical Engineering*, Vol. 3(1), 89-98.

Rao, M.V.S., Ramesh, V.K., Rames, M.N.V., and Rao, B.S. (2013), Effect of Copper Doping on Structural, Dielectric and DC Electrical Resistivity Properties of $BaTiO_3$, *Advance Material Physical Chemistry*, Vol. 3, 77–82.

Saikat, M. Mousumi B., Siddhartha M., Singh, P.K. (2013), Synthesis and Characterization of Cobalt Oxide Doped Barium Strontium Titanate, *Jounal of Austral Ceramics Society*, Vol. 49 (1), 79–83.

Sheela. D. and Jha. A. K. (2009), Structural, Dielectric and Ferroelectric Properties of Tungsten Substituted Barium Titanate Ceramics. Asian *Journal of Chemistry*, Vol. 21(10), 117-124.

Vitayakorn, N. (2006), Dielectric Properties of Bismuth Doped Barium Titanate (BaTiO3) Ceramics, Journal of Applied Sciences Resources, Vol. 2 (12), 1319–1322.

Yun, S., Wang X., Li,B., and Xu D. (2007), Dielectric Properties of Ca-Substituted Barium

Strontium Titanate Ferroelectric Ceramics, Journal of Solid State Community, Vol. 143, 461–465.